**Structural Engineering and Mechanics**, *Vol. 64, No. 1 (2017) 135-143*
DOI: https://doi.org/10.12989/sem.2017.64.1.135


# Shear-strengthening of RC continuous T-beams with spliced CFRP U-strips around bars against flange top

Chaoyang Zhou[1a], Da Ren[*2] and Xiaonian Cheng[1b]

[1]*School of Civil Engineering, Central South University, 68 Shaoshannan Road, P.R. China*
[2]*School of Civil Engineering, Guangzhou University,230 Waihuanxi Road, P.R. China*

*(Received November 18, 2016, Revised August 16, 2017, Accepted August 17, 2017)*

**Abstract.** To upgrade shear performance of reinforced concrete (RC) beams, and particularly of the segments under negative moment within continuous *T*-section beams, a series of original schemes has been proposed using carbon fibre-reinforced polymer (CFRP) *U*-shaped strips for shear-strengthening. The current work focuses on one of them, in which CFRP *U*-strips are wound around steel bars against the top of the flange of a *T*-beam and then spliced on its bottom face in addition to being bonded onto its sides. The test results showed that the proposed scheme successfully provided reliable anchorage for *U*-strips and prevented premature onset of shear failure due to FRP debonding. The governing shear mode of failure changed from peeling of CFRP to its fracture or crushing of concrete. The strengthened specimens displayed an average increase of about 60% in shear capacity over the unstrengthened control one. The specimen with a relatively high ratio and uniform distribution of CFRP reinforcement had a maximum increase of nearly 75% in strength as well as significantly improved ductility. The formulas by various codes or guidelines exhibited different accuracy in estimating FRP contribution to shear resistance of the segments that are subjected to negative moment and strengthened with well-anchored FRP U-strips within continuous T-beams. Further investigation is necessary to find a suitable approach to predicting load-carrying capacity of continuous beams shear strengthened in this way.

**Keywords:** beams; reinforced concrete; FRP; shear; strengthening; anchorage

## 1. Introduction

Fiber-reinforced polymer (FRP) fabric has been widely used in the repair of reinforced concrete structures due to excellent corrosion resistance, high strength-over-weight ratio and ease of installation (Hollaway 2010, Panda *et al*. 2013, Yurdakul and Avsar 2015, Deng *et al*. 2016). Usually FRP sheets (FRPs) is externally bonded (EB) to surface of RC beams for shear strengthening. A number of experimental and/or theoretical studies have been done on this subject over the last two decades (Khalifa *et al*. 1998, Triantafillou and Antonopoulos 2000, Lees *et al*. 2002, Deniaud and Roger Cheng 2003, Chen and Teng 2003, Bousselham and Chaallal 2008, Al-Mahaidi and Kalfat 2011, Mofidi *et al*. 2014).

As an EB FRP configuration, complete wrapping is an effective scheme. For a beam with *T*-shaped cross-section (*T*-beam), however, the flange will stop FRPs from reaching the top for a closed hoop. In particular, if the *T*-beam is beneath a wall, the wall above it will also prevent FRP from enclosing, which further makes the scheme impractical. Therefore, EB FRP *U*-shaped strips (i.e., *U*-jackets) are more popularly used. Nevertheless FRP *U*-strips are prone to debonding from beam sides which may eventually cause a brittle failure. This is especially true when the portions strengthened with *U*-strips are near the supports of a continuous *T*-beam, where both shear force and negative bending moment approach maximum. In such case, a critical shear crack generally starts from the tension zone at the upper part of the beam, where the crack is usually wider. As all *U*-strips have an upward opening, their ends are also located in that zone. Thus, those intersected by the crack will have a relatively short bonding length and debonding will arise more easily. Since the flange will further limit access of the *U*-strips to its top, some may even be intersected by no cracks; the effect of strengthening may get even worse. The prevention of such debonding failure becomes a key problem to tackle in the application of FRP *U*-strips to shear strengthening.

A few codes (e.g., ACI 440.2R-08, FIB 2001, ISIS 2001, TR55 and CNR-DT200R1) and relevant literature recommend anchoring *U*-strips at their ends against FRP debonding. A variety of anchoring systems have been developed based on extensive experimental studies (Sato 1997, Khalifa and Nanni 2000, Schuman 2004, Hoult and Lees 2009, Galal and Mofidi 2010, Belarbi *et al*. 2012, Mofidi *et al*. 2014, Triantafillou and Koutas 2013, Baggio *et al*. 2014, EI-Saikaly 2015, Chen *et al*. 2016). For instance, Sato *et al*. (1997) anchored the end of the FRP with steel plates bolted to concrete. Khalifa and Nanni (2000) proposed a so-called *U*-anchor system, in which FRP *U*-strips are fixed by winding the ends around rods and pasting to a preformed groove near the reentrant of the

∗Corresponding author, Associate Professor
E-mail: renda20099@126.com
[a]Professor
[b]M.Sc.



ISSN: 1225-4568 (Print), 1598-6217 (Online)

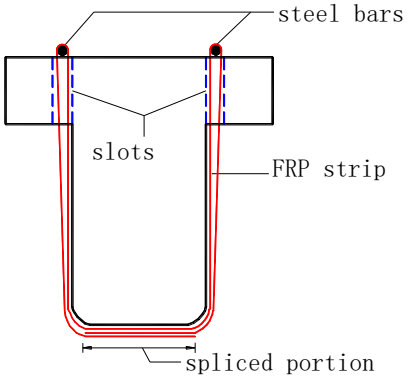


Fig. 1 Configuration for the proposed scheme

beams. Schuman(2004) employed GFRP plate plus steel bolts to press CFRP *U*-strips at ends in the chamfer region of continuous bridge *T*-beams. Galal and Mofidi (2010) wrapped each end of dry CFRP sheets separately around a steel rod bolted to the web-flange junction of a *T*-beam in an unbonded *U*-jacket anchoring system. Belarbi *et al*. (2012) reported a sandwich-panel anchoring system, in which two CFRP plates clamped the ends of the FRP sheets and secured with steel bolts. Several researchers (Koutas and Triantafillo 2013, Baggio *et al*. 2014, EI-Saikaly *et al*. 2015) applied FRP spike anchors to shear strengthening. In the tests on rectangular beams from Baggio *et al*. (2014), there seemed to be little gain in the shear capacities of the beams strengthened with the modified spike-anchor system. In a similar way to Baggio's, EI-Saikaly *et al*. (2015) retrofitted their *T*-beams with rope-anchored *L*-shaped strips, which obtained a greater increase in shear resistance. Chen *et al*. (2016) anchored the end of FRP *U*-strips in a manner of combining *U*-anchor by khalifa and Nanni and self-locked-around-bars configuration by the authors (2013), and compared it with the spike-anchor system.

It is clear that anchoring FRP *U*-strips at ends has been widely accepted. But the efficacy for various anchorages remains controversial against limited database. Some schemes can be used in laboratory without difficulty but hard to implement on site and, above all, the investigation is in particular shortage on their reliability in shear rehabilitation of continuous beams. The main objectives of this work are as follows: 1) to present a new system for anchoring FRP *U*-strips that will be practical and effective; in the case that an upper wall sits on a beam, its installation needs to drill through flange only and not to penetrate the wall, which makes it more feasible than complete wrapping; 2) to examine the scheme's efficiency in shear repair of negative-moment segments in continuous *T*-beams; 3) to check if existing code formulas apply to evaluating FRP's contribution to shear strength of *T*-beams bonded with end-anchored FRP *U*-strips and subjected to negative moment.

## 2. Anchoring scheme and process

Fig. 1 shows the basic configuration for the proposed scheme. First, make long narrow openings through flange just beside the web-flange junction; the slots should be slightly longer than the width of a *U*-strip. Second, have the *U*-strip encompass the web, pass its two ends through the slots, and wind them around two separate steel bars on the top of the flange respectively. Third, get through the corresponding slots back along web side to the beam bottom and spliced at soffit with epoxy resin. The particular process of installation is described as follows.

Prior to casting, slots were preformed for all specimens of strengthened beam segment. The length, width, and height of each slot were 50 plus, 20, and 75 mm (equal to the thickness of flange), respectively. The corners of section were rounded and surface preparation (e.g., sanding) was made along the route to bond CFRP strips. CFRP sheets were cut into strips. The mixture of adhesive was then prepared and uniformly pasted on the areas to bond strips. As shown in Fig. 1, two separate steel bars with smooth surface and a 12 mm diameter was put lengthwise onto the top of beam flanges right above the two rows of preformed slots. Every single CFRP *U*-strip was then impregnated with epoxy, and its ends were passed through the slots, wound around the two separate bars on the flange top, inserted back through, pulled together and finally spliced at the bottom of the web (spliced length is nearly equal to the web width of 150 mm), followed by surface-rolling several times in the fiber direction for extruding bubbles.

It needs to be noted that the diameter of the bars was determined according to the condition that they would not yield before the FRPs attained the ultimate tensile strength. In practice, to meet the requirements for usage and appearance, bars can be made flush with floor by cutting groove within concrete cover, or embedded into an additional cover in the case of a thin flat plate.

With enough spliced length, this scheme is expected to work effectively against debonding failure without a reduction of depth over which *U*-strips are bonded at beam sides.

## 3. Experimental program

### *3.1 Specimens*

In a RC continuous beam, each portion near supports is often subjected to combinations of significant shear and negative bending moment, being the crucial part to be strengthened for shear. As noted earlier, EB FRP *U*-strips will debond from beam sides more easily due to the adverse propagation of the critical shear crack under negative moment. Unfortunately, few studies focused on shear repair of such special portions. This paper added to database such examples by experiments.

The *T*-beams to be tested were all 2000 mm long, 300 mm deep with a 300-mm wide flange and 150-mm wide web. As shown in Fig. 2, one *T*-beam consisted of two testing segments that shared an assisting part in the middle. Each segment plus the assisting part was treated as a single specimen, thus each *T*-beam actually contained two specimens, which were experimented in sequence by adjusting the locations of the supports and the loading position. The purpose of such design is to eliminate to the

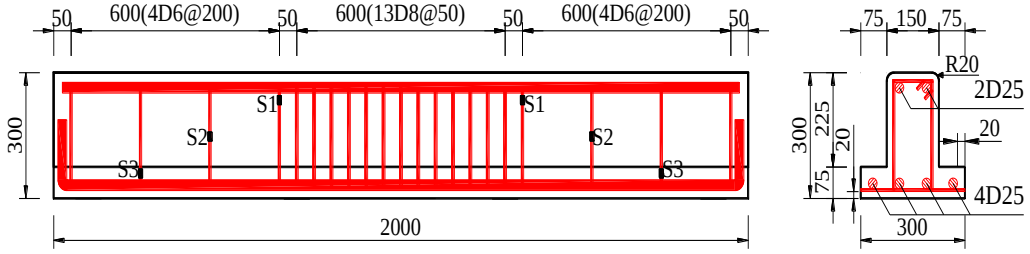


(a) dimensions and reinforcement (*D*=diameter and @ denotes spacing)

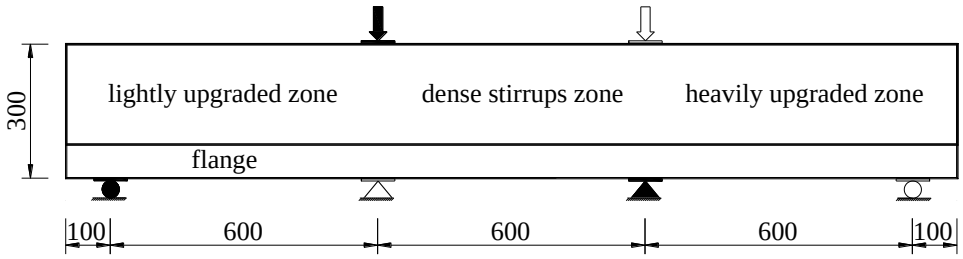


(b) two-stage test scheme

Fig. 2 Details of the specimens and testing program (all dimensions in mm)

Table 1 Properties of steel reinforcement bars

| Diameter of reinforcement bars (mm) | Yield strength (MPa) | Tensile strength (MPa) | Young's modulus (GPa) |
|---|---|---|---|
| 6.5 | 343 | 467 | 210 |
| 8 | 350 | 543 | 210 |
| 25 | 403 | 597 | 200 |

greatest extent the influence of variation of concrete strength, which is often inevitable if the concrete is not produced from the same batch.

All specimens had an identical shear span-to-depth ratio $\lambda$ of 2.13 and the same steel reinforcement with a 20-mm thick cover. The longitudinal steel bars were overdesigned in order to prevent flexural failure. The steel stirrups with 6.5 mm diameter and 200 mm spacing were provided for the portion to be strengthened, corresponding to a percentage of 0.221%. The assisting part had more densely spaced stirrups, namely, an 8 mm diameter and 50 mm spacing. Table 1 presented the mechanical properties measured for reinforcement bars.

Five specimens were tested in this experiment, including one unstrengthened as reference and four strengthened (see Table 2). A set of rules for numbering is used so that each specimen can be simply identified. The first capital letter denotes the shape of cross section of a specimen, followed by a small letter representing the grade of concrete strength, and then followed by an Arabic number representing the ratio of shear-span to depth. The second capital letter is used to recognize the way of anchoring *U*-strips. The three digits next to it denote the layers of FRP strip on one side of beam, width of an individual FRP strip (1 for 25 mm and 2 for 2×25 mm), and center-to-center spacing of adjacent FRP strips (1 for 100 mm and 2 for 2×100 mm), respectively. For example, $Tc_2S_{212}$ represents a *T*-section beam with a concrete strength of 29.1 MPa and a shear span-to-depth ratio of 2.13. The beam is strengthened with spliced FRP *U*-strips (splice as a key word distinguishing from other way). There are two layers of 25 mm wide strips on each side of the beam, and the adjacent strips are spaced at 200 mm from one strip center to another. It should be noted that the current investigation is only one part of a large experimental program which actually contains several batches of concrete, and the strength for each batch is represented with a particular letter when symbolizing specimens. For example, Letter "*c*" represents 29.1 MPa, or the strength value for this batch of concrete as mentioned above.

As listed in Table 2, primary variables involved CFRP content and details of the strips. Despite the same layer and thickness, there is change in either width or centre-to-centre spacing of the CFRP strips for different strengthened specimen. According to the manufacturer, the CFRP sheet is 0.167 mm thick, with a tensile strength of 3450 MPa, a Young's modulus of 230 GPa and an ultimate tensile strain of 0.015.

### *3.2 Testing*

To simulate behavior of negative-moment segments in continuous *T*-beams strengthened with end-anchored FRP *U*-strips, all specimens were tested in three-point bending and with their flanges in tension zone (see Fig. 2(b)). Contrary to typical tests on simple *T*-beams, such distribution of internal forces conformed to real situation in that key region. The loading point may be regarded as a support (e.g., column) of a continuous beam and the reactions at two simple supports as shear forces at its contra flexural points.

The width of the steel pads for bearing at the supports and loading point was 60 mm and 120 mm, respectively. A hydraulic jack was used to exert downward load at midspan. Fig. 2(a) and 3 show the locations of strain gauges for stirrups and for CFRP strips, respectively. They are

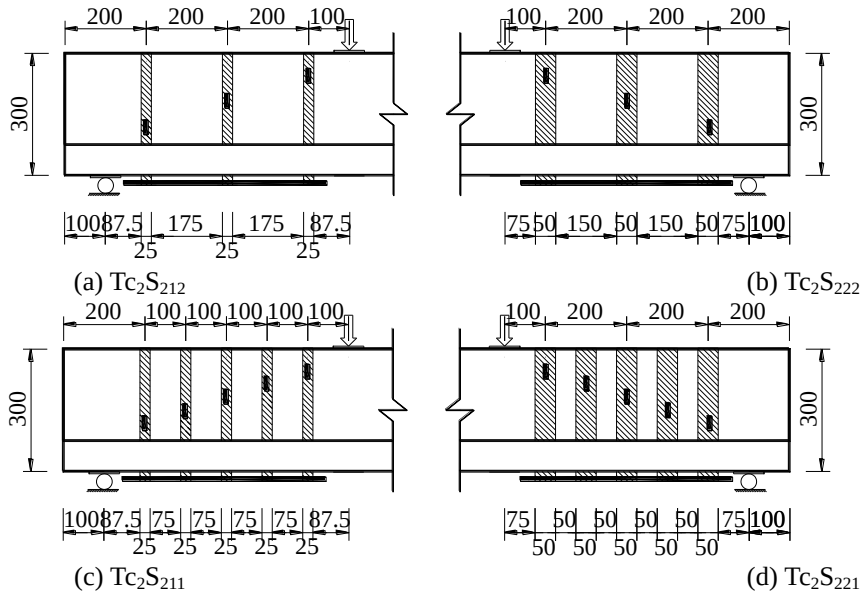


Fig. 3 CFRP detailing and strain-gauge locations (all dimensions in mm)

Table 2 Parameters for specimens plus test results

| Beam | $f_{cu}$* (MPa) | CFRP parameters* | | | | Characteristic shear* | | | Failure modes* |
|---|---|---|---|---|---|---|---|---|---|
| | | $n$ | $w_f$ (mm) | $s_f$ (mm) | $\rho_{fv}$ (‰) | $P_{cr}$ (kN) | $P_u$ (kN) | Enhancement (%) | |
| $Tc_2$ | 29.1 | 0 | 0 | 0 | 0 | 65 | 135 | 0 | *Cr* |
| $Tc_2S_{212}$ | 29.1 | 2 | 25 | 200 | 0.56 | 65 | 195.2 | 44.4 | *R* |
| $Tc_2S_{222}$ | 29.1 | 2 | 50 | 200 | 1.11 | 70 | 215.2 | 59.3 | *R+Cr* |
| $Tc_2S_{211}$ | 29.1 | 2 | 25 | 100 | 1.11 | 80 | 215.5 | 59.3 | *R+Cr* |
| $Tc_2S_{221}$ | 29.1 | 2 | 50 | 100 | 2.22 | 80 | 235.3 | 74.1 | *Cr* |

*$f_{cu}$= cubic compressive strength of concrete;
$n$= layers of FRP strip bonded to one beam side; $w_f$= width of an individual FRP strip; $s_f$= center-to-center spacing of adjacent FRP strips; $\rho_{fv}$= FRP reinforcement ratio;
$P_{cr}$= cracking shear force; $P_u$= ultimate shear force; shear force is equal to one half of the applied load; Enhancement ratio of $P_u$ for the strengthened beam relevant to that for the control beam;
*Cr*=concrete crushing in compression zone; *R*=FRP rupture.

approximately positioned at the straight connecting the loading point to the support.

For convenience of description below, the measured points from the midspan on for FRP strips are labeled F1 to F5 (or F1, F3 and F5 in case of three strips only) and for steel stirrups labeled S1 to S3 in sequence. In addition, displacements at midspan and supports were recorded and crack propagations were marked during loading.

## 4. Test results and discussions

### *4.1 Shear strength and failure modes*

The test results for all five specimens are summarized in Table 2. The table gives the cracking shear forces at which initial shear cracks occurred, ultimate shear forces, and the enhancement in shear capacity due to CFRP *U*-strips as a percentage of the control beam's. In addition, the failure mode for each specimen is also presented.

As shown in Table 2, all specimens of strengthened beams displayed noticeable promotion in shear capacity. On average the rise percentage was 59.3%. From the table, it can be seen that ultimate shear force rose as the CFRP ratio increased. Beam $Tc_2S_{221}$ achieved a maximum gain in shear strength of 74.1% over the control beam, $Tc_2$. This was mainly ascribed to its relatively heavy content and uniform distribution of CFRPs. It led to a high contribution of FRP to shear capacity and meanwhile produced strong restraint to concrete in compression, which indirectly enlarged contribution of concrete to shear resistance.

It needs to be noted that in most cases, beams shear-strengthened with EB FRP *U*-strips will experience premature FRP-debonding failure, giving rise to limited improvement in shear-carrying capacity. In our pilot tests exerting negative moments along with shear to *T*-beam segments (Zhou *et al*. 2012), a piece of *U*-sheet, continuous in both circumferential and longitudinal direction, was bonded to three surfaces of a specimen without additional anchors. As expected, premature debonding led to poor upgrading effect and the shear resistance increased only by 4% over its reference without strengthening. With the same content of CFRP, however, *U*-strips with similar anchorage to the proposed configuration helped an otherwise identical specimen to achieve an increase of 56%, indicating a much higher efficacy of strengthening. Also owing to the reliable anchorage, all four segments strengthened here can carry further load after debonding until ultimate shear forces much greater than control one. Hence debonding is no more a typical mode of failure since it does not lead to final failure immediately.

The control beam featured typical crushing of the compressed concrete at shear failure. Among the strengthened beams, Beam $Tc_2S_{212}$ with relatively small CFRP content failed by CFRP rupture. Beams $Tc_2S_{211}$ and

$Tc_2S_{222}$ experienced CFRP rupture and nearly in the meantime crushing of concrete beneath the loading point at failure. With a largest amount of CFRP reinforcements, Beam $Tc_2S_{221}$ failed by concrete crushing, followed by just a shred of FRP fracture as a secondary effect. The compression concrete near the loading pad even bulged outside at ultimate for the strong confinement by the FRP strips. These results indicated that the amount and distribution of CFRPs play an important role on which mode of failure will take place for a specific strengthened beam. Of course, the failure mode results from a combination of multifactor actions. It may be inferred that with a higher concrete strength, specimen $Tc_2S_{221}$ might fail by CFRP rupture and meantime achieve greater promotion in shear capacity than 74.1%.

### *4.2 Crack propagation and patterns*

For the control beam, $Tc_2$, as the applied load increased up to 130 kN (i.e., the corresponding shear force was 65 kN), an initial inclined crack appeared on the web near the flange-web junction. Then new cracks occurred successively and some propagated towards the load point until a critical inclined crack formed (Fig. 4).

For the strengthened Beams $Tc_2S_{222}$, $Tc_2S_{211}$, and $Tc_2S_{221}$, initial cracking occurred at a somewhat higher load compared to the control beam, $Tc_2$. Their cracking shear forces were enhanced from 65 for $Tc_2$ to 70, 80, and 80 kN, respectively. But for Specimen $Tc_2S_{212}$, with sparsely distributed and thus a relatively small amount of FRPs, the cracking shear remained nearly the same as $Tc_2$. As the applied force reached 180 to 200 kN, splitting cracks were seen in the flanges due to thin cover and large diameter of longitudinal reinforcement bars. This reduced so-called dowel action provided by the steel reinforcement bars and to some extent impaired the anchoring effect for CFRP, resulting in an adverse influence on shear resistance. Still other minor cracks were observed in close proximity of the slots owing to stress concentration.

As load further increased, new cracks were frequently found in the mid-web between strips, and the initial cracks diagonally extended towards the top and bottom edge of the beam. Subsequently the critical shear crack formed, being at about 30 degrees with respect to the longitudinal axis. The beam strengthened with a larger amount of FRPs seemed to have a greater inclination of critical shear crack given that other parameters were identical (Fig. 4).

It was noted that the cracking shear for $Tc_2S_{211}$ with FRP-strips spaced at 100 mm was larger than that for $Tc_2S_{222}$ with 200-mm spacing, despite the same fiber content. But it was similar to $Tc_2S_{221}$ with double content of fiber yet equal spacing of FRP strip. This suggested that relatively uniform distribution of strip is beneficial to restraining crack propagation.

### *4.3 Deflection and strain responses*

The load-midspan deflection curves are depicted in Fig. 5. All five beams initially had nearly the same stiffness. However, the beams' stiffness started to diverge at a load ranged from 130 to 160 kN, during which initial inclined cracks were observed. In comparison, the beams with less FRP content had a faster reduction of stiffness. As an extreme, the control beam without CFRP strips displayed the most obvious loss of stiffness since the critical shear crack formed. It may be inferred that CFRP *U*-strips anchored in the proposed way were effective in suppressing cracking and reducing deflection. Moreover, it seemed that the more FRP reinforcement a beam had the better ductility it would exhibit. For instance, of all five beams, Beam $Tc_2S_{221}$ had the largest deflection at failure and developed an apparent plateau due to its high FRP reinforcement ratio.


(a) $Tc_2$ (b) $Tc_2S_{212}$ (c) $Tc_2S_{222}$

(d) $Tc_2S_{211}$ (e) $Tc_2S_{221}$

Fig. 4 Failure profiles and crack patterns

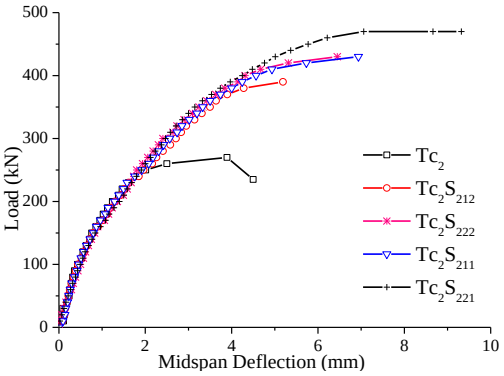


Fig. 5 Load-deflection curves

Fig. 6 shows load-strain curves for Beams $Tc_2S_{212}$ and $Tc_2S_{221}$, whose CFRP content was either the least or the most. As can be seen, strains increased very slowly in both CFRP strips and steel stirrups before the initial shear cracks emerged. From initial-cracking on, the CFRP strips and steel stirrups crossed by inclined cracks displayed a steady increase in strain level. This implied that the crack opening prompted both CFRPs and steel stirrups to resist shear more actively. Take Beam $Tc_2S_{221}$ for example. Prior to cracking, strains in all strips stayed below 150 $\mu\varepsilon$. After cracking, the strain value kept on growing. Furthermore, it seemed that the strain response in CFRP strips was more sensitive to formation of the critical shear crack than that in steel stirrups. As the load ranged from 320 to 360 kN, during which the critical crack formed, the strains in Strips F3 and F4 increased rapidly by 1200 and 800 $\mu\varepsilon$, respectively. Whereas Stirrup S2, at the very middle of shear span, still kept a gradual increase in strain of about 400 $\mu\varepsilon$ only. In fact, the maximum strain in all CFRP strips was much higher than that in the stirrups after the critical crack occurred. This was also verified by Miyauchi *et al*. (1997). Incidentally, as compared to control beam, all strengthened beams had a lower strain value in Stirrup S2 under the same load level, implying that CFRP did share partial shear.

For Beams $Tc_2S_{212}$, $Tc_2S_{222}$, $Tc_2S_{211}$, and $Tc_2S_{221}$, the highest level of strain recorded in FRP were recorded at 9769, 8335, 7273, and 5057 $\mu\varepsilon$, respectively. Apparently, the beam with the largest FRP reinforcement ratio (i.e., $Tc_2S_{221}$) had the least value of the maximum strain in FRP. This showed that the efficacy of utilization of FRP tended to decline with the increasing FRP content. In addition, the maximum strain took place in the strip closest to the midmost of shear span. For instance, Fig. 6(b) showed that Strip F3 had a larger strain value over Strip F5. The case is also true among steel stirrups. Stirrup S2, e.g., located in the middle portion, also developed a strain level higher than Stirrups S1 and S3 during the entire loading process.

It is an interesting finding from Fig. 6(a) that Strip F2 in Beam $Tc_2S_{212}$ seemed to experience several transient decreases in strain at loads roughly from 260 to 330 kN. Shortly after the little drops, the strip strain regained status quo ante and continued to grow again. This may be a unique feature for beams strengthened with FRP *U*-strips well anchored. At the very moment of debonding, a sudden decrease in strain occurred locally in the FRP strip that just

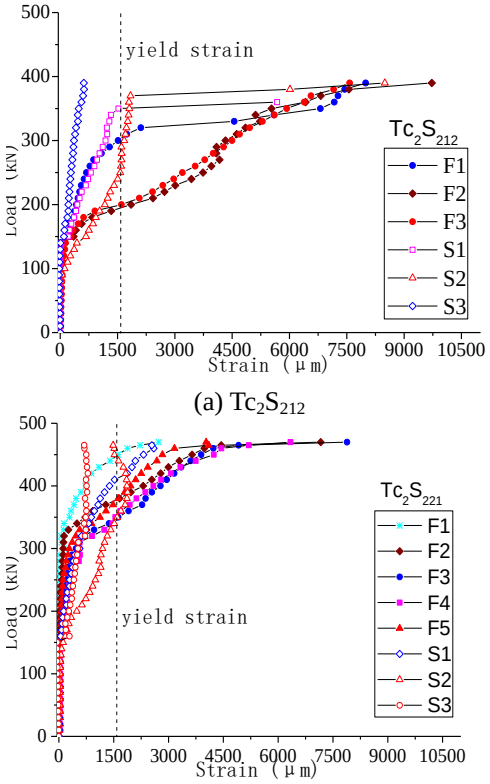


(a) $Tc_2S_{212}$

(b) $Tc_2S_{221}$

Fig. 6 Load-strain curves

debonded. With the help of end anchorage, however, the strain in that strip was able to reach the same magnitude as just before its debonding and then proceed to increase. While for Beam $Tc_2S_{221}$, the above feature appears not so obvious (Fig. 6(b)). This is mainly due to the fact that the FRP-strain gauges failed to capture the precise locations where debonding occurred.

### *4.4 Estimate of FRP's shear contribution*

To calculate shear-carrying capacity of an EB FRP-strengthened beam, most codes or researchers generally follow the rule of simple superposition, namely

$$V_u = V_c + V_s + V_f \tag{1}$$

Where $V_u$ is the beam's shear strength, $V_c$, $V_s$ and $V_f$ are the contribution of concrete, internal web reinforcement (e.g., steel stirrups) and external FRP reinforcement, respectively. $V_c$ and $V_s$ may also be jointly denoted as $V_{cs}$. Since the three components are interrelated and dependent, it is hard to exactly estimate every single one. An approximate treatment widely accepted in literature is to calculate $V_{cs}$ and $V_f$ separately. Note that $V_{cs}$ value may be obtained using relevant provisions for conventional reinforced concrete beams (with steel transverse reinforcement only) available in existing codes. Thus the evaluation of FRP's shear contribution $V_f$ becomes the major concern in determining the shear strength $V_u$.

From the truss theory, a general expression to compute $V_f$ can be derived as

$$V_f = 2nt_f w_f \varepsilon_{fe} E_f d_f (cot\theta + \cot\beta)\sin\beta / s_f \quad (2)$$

where $n$=number of FRP layers; $t_f$=thickness of a single FRP layer; $w_f$=width of an individual FRP strip; $E_f$= Young's modulus of FRP; $\varepsilon_{fe}$=effective strain in FRPs; $d_f$=effective height of FRP on the beam sides; $\beta$=angle of fiber orientation to the longitudinal axis of the beam; $\theta$=inclination of the critical shear crack; and $s_f$=center-to-center spacing between two adjacent strips.

Many existing codes, with their models based on the same truss theory, take a formally similar expression to Eq. (2), including the ACI 440.2R-08, TR55 2012, ISIS 2001, HB 305, CNR-DT 200 R1, JSCE 2001, etc. In these models, the differences are primarily from such aspects as safety factors adopted and the way of treating certain variables. For instance, different is treatment on the inclination of critical shear cracks (i.e., $\theta$). Codes HB 305 and CNR-DT 200 R1 include the crack angle $\theta$ explicitly, while others (e.g., ACI 440.2R-08) do not, which can be understood to take a conservative value of 45 degrees.

The key difference, however, lies in the determination of effective or average strain in FRPs (i.e., $\varepsilon_{fe}$). Each code has its own approach to deciding $\varepsilon_{fe}$ and most of them give two distinct expressions, distinguishing between the configuration of full wrapping and that of *U*-jacketing or side bonding. One can refer to relevant codes for particular expressions. The test results have already shown that *U*-jacketing with special end-anchorage proposed in this paper is a reliable configuration just as full wrapping. So it is supposed that existing code formulas on $\varepsilon_{fe}$ and thus the resulting $V_f$ for full wrapping might be also applicable to the new configuration. It should be noted that these formulas are generally developed based on data from classical tests on simple beams with rectangular cross-section. Nevertheless in the present study, all FRP-strengthened beams were designed and tested targeting the portions under negative moment in continuous T-beams. Therefore, it need at least to be verified through calculation whether the existing formulas apply to the case studied here.

Table 3 presented the observed values of $V_f$ in the strengthened beams and the predicted ones by existing codes. For the purpose of comparison, no safety factors were considered in the use of these code formulas. The observed $V_f$ was obtained by subtracting $V_{cs}$ from the recorded shear strength $V_u$. $V_{cs}$ is taken as equal to the shear capacity of the control beam, which can be calculated by existing code provisions for conventional reinforced concrete members when its test value is not available.

As shown in Table 3, on average, the models suggested by codes TR55 2012 and ACI440.2R-08 made overly conservative predictions. This is partially because the two codes both set a strict limit to the level of effective strain that can be developed in FRPs. In Code ACI440.2R-08, e.g., the upper bound for $\varepsilon_{fe}$ is 0.004 and in British code this value is even smaller. By comparison the predictions were less conservative by the models from Codes CNR-DT 200 R1 and ISIS 2001. Averagely, Codes HB305 and JSCE 2001 tended to overestimate values of $V_f$ compared with its observed values. For the case of $Tc_2S_{221}$, the overestimation of some models (e.g., HB305, CNT-DT-200R1. JSCE2011) can be attributed to the fact that the experimental shear strength was bounded by the compression failure of concrete instead of FRP rupture.

Table 3 Comparison between the observed and predicted FRP contribution to shear strength

| specimen | $V_{f,test}$ (kN) | $V_{f,calc}$* (kN) | | | | | | |
|---|---|---|---|---|---|---|---|---|
| | | ACI440.2R-08 | TR55-2012 | FIB 2001 | ISIS 2001 | HB 305 | CNR-DT 200R1 | JSCE 2001 |
| $Tc_2S_{212}$ | 60.2 | 20.7 | 17.8 | 27.9 | 36.5 | 48.4 | 31.5 | 55.4 |
| $Tc_2S_{222}$ | 80.2 | 41.0 | 35.3 | 53.0 | 58.9 | 88.6 | 56.8 | 88.4 |
| $Tc_2S_{211}$ | 80.5 | 41.0 | 35.3 | 53.0 | 58.9 | 88.6 | 57.2 | 88.4 |
| $Tc_2S_{221}$ | 100.3 | 82.0 | 70.6 | 86.2 | 95.7 | 191.7 | 120.6 | 125.2 |
| $\mu$* | — | 0.55 | 0.47 | 0.66 | 0.76 | 1.23 | 0.79 | 1.09 |
| COV | — | 0.362 | 0.363 | 0.245 | 0.191 | 0.386 | 0.370 | 0.123 |

*$\mu$ denotes the mean of ratios of the theoretically computed $V_f$ to its observed values, and *COV* represents the coefficient of variation for the ratios;
$V_{f,test}$ = observed contribution of FRP to shear resistance in tests, which is obtained by removing $V_c$ and $V_s$ from the observed shear strength. $V_c$+$V_s$ (i.e., shear contribution provided by stirrups plus concrete) is taken as equal to the observed shear capacity of control beam;
$V_{f,calc}$ = calculated contribution of FRP to shear resistance by various code models.

It needs to be stressed that no partial safety factors are considered in the predictions by all code models. As these models generally adopt different safety factors, it makes no sense to judge conformity of a certain model with test results by the mean of ratios of its predicted values to the observed.

In terms of coefficient of variation, the formula recommended by JSCE 2001 seems to predict the tendency of change of $V_f$ with FRP allocation better than other models discussed here. In view of the fairly limited test data, however, it is too early to make definite decision on accuracy of these code models. More experiments will be needed aiming at the negative-moment portions of continuous *T*-beams strengthened in shear with well-anchored FRP *U*-strips. In addition, research is necessary to establish a relatively refined model for $V_f$ and then $V_u$.

## 5. Conclusions

Debonding is a common phenomenon in reinforced concrete beams shear strengthened with EB FRP *U*-shaped strips. It will be even more serious for the segments that are subjected to negative moment within a continuous *T*-beam. In order to prevent shear failure caused by FRP debonding, this paper presents a new scheme for anchoring FRP *U*-strips. In this scheme, *U*-strips are wound around additional bars against top of flange and then spliced at bottom of web in addition to side bonding. Based on the experimental results, the main conclusions were drawn as follows:

- The proposed anchorage is applicable to beams with *T*-shaped section, even if there exists a wall above them.

• The test results demonstrated that the proposed scheme was effective in anchoring CFRP *U*-strips and thus obtaining good effect of strengthening. For all *T*-beams strengthened, the shear capacity increased by an average of nearly 60% and a maximum up to close 75% as compared to the control specimen.

• All specimens failed by either CFRP rupture or concrete crush, depending on how CFRP is added and arranged. For those strengthened with *U*-strips anchored in the suggested way, shear failure due to premature debonding were well avoided, implying debonding was no more a typical mode of failure. Even if debonding happened, in fact, loads can be further increased until other factors caused ultimate failure.

• Cracking shear and stiffness for all the strengthened beams had been enhanced to some extent. Their ductility had also been improved, especially for specimens with higher content and denser distribution of CFRP strips. This revealed that with the help of well-anchored CFRP, beams can exhibit more ductile behavior of shear failure than unstrengthened one.

• In calculating the contribution of FRP to shear capacity, available code formulas are mainly based on test results of simple rectangular beams with complete wrapped FRP. They have different accuracy of prediction for negative-moment segments strengthened with end-anchored *U*-jackets. In terms of coefficient of variation, the method recommended by JSCE 2001 seems to predict the tendency of change of FRP's contribution with its allocation better than other models.

• Note that existing test data are limited, it is necessary to make further investigation on shear strengthening of continuous *T*-beams with well-anchored FRP *U*-strips.

## Acknowledgments

This research is supported and/or sponsored by the Natural Science Foundation of P.R.China (Project No. 50778176, 51378507), the Natural Science Foundation of Hunan Province, PR China (Project No. 08JJ3105), and Excellent Teacher's Grant of Central South University (Project No. 2013JSJJ019).

## References

ACI-440.2R (2008), "Guide for the design and construction of externally bonded FRP systems for strengthening concrete structure", ACI-440.2R, American Concrete Institute, Farmington Hills, Michigan, USA

Al-Mahaidi, R. and Kalfat, R. (2011), "Investigation into CFRP plate end anchorage utilising uni-directional fabric wrap", *Compos. Struct.*, **93**(2), 821-830.

Baggio, D., Soudki, K. and Noel, M. (2014), "Strengthening of shear critical RC beams with various FRP systems", *Constr. Build. Mater.*, **66**, 634-644.

Belarbi, A., Bae, S.W. and Brancaccio, A. (2012), "Behavior of full-scale RC T-beams strengthened in shear with externally bonded FRP sheets", *Constr. Build. Mater.*, **32**(4):27-40.

Bousselham, A. and Chaallal, O. (2008), "Mechanisms of shear resistance of concrete beams strengthened in shear with externally bonded FRP", *J. Compos. Construct.*, **12**(5), 499-512.

Chen, G.M., Zhang, Z., Li, Y.L., Li, X.Q. and Zhou, C.Y. (2016), "T-section RC beams shear-strengthened with anchored CFRP-U strips", *Compos. Struct.*, **144**,57-79.

Chen, J.F. and Teng, J.G. (2003), "Shear capacity of fiber-reinforced polymer-strengthened reinforced concrete beams: Fiber reinforced polymer rupture", *J. Struct. Eng.*, **129**(5), 615-625.

CNR-DT-200R1 (2013), "Guide for the design and construction of externally bonded FRP systems for strengthening existing structures", CNR-DT-200R1, Advisory Committee on Technical Recommendations for Construction, National Research Council, Rome, Italy.

Deng, J.D., Liu, A.R., Huang, P.Y. and Zheng, X.H. (2016), "Interfacial mechanical behaviors of RC beams strengthened with FRP", *Struct. Eng. Mech.*, **58**(3), 577-596.

Deniaud, C. and Roger Cheng, J.J. (2003), "Reinforced concrete T-beams strengthened in shear with fiber reinforced polymer sheets", *J. Compos. Construct.*, **7**(4), 302-310.

El-Saikaly, G., Godat, A. and Chaallal, O. (2015), "New anchorage technique for FRP shear- strengthened RC T-beams using CFRP rope", *J. Compos. Construct.*, **19**(4), 04014064-1-11.

FIB (2001), "Externally bonded FRP reinforcement for RC structures", Task Group 9.3 FRP (Fibre Reinforced Polymer) Reinforcement for Concrete Structures, Bulletin No.14, Federation Internationale du Beton (fib), Lausanne, Switzerland.

Galal, K. and Mofidi, A. (2010), "Shear strengthening of RC T-beams using mechanically anchored unbonded dry carbon fiber sheets", *J. Perform.Constr. Facil.*, **24**(1), 31-39.

HB305 (2008), *Design Handbook for RC Structures Retrofitted with FRP and Metal Plates: Beams and Slabs*, Published by Standards Australia, Sydney, Australia.

Hollaway, LC. (2010), "A review of the present and future utilisation of FRP composites in the civil infrastructure with reference to their important in-service properties", *Constr. Build. Mater.*, **24**(12), 2419-2445.

Hoult, N.A. and Lees J.M. (2009), "Efficient CFRP strip configurations for the shear strengthening of reinforced concrete T-beams", *J. Compos. Construct.*, **13**(1), 45-52.

ISIS (2001), Design Manual No.4: Strengthening Reinforced Concrete Structures with Externally-bonded Fiber Reinforced Polymers, Intelligent Sensing for Innovative Structures, Canada.

JSCE (2001), "Recommendations for upgrading of concrete structures with use of continuous fiber sheets", Concrete Engineering Series 41 (English Version), Japan Society of Civil Engineers, Tokyo, Japan.

Khalifa, A. and Nanni, A. (2000), "Improving shear capacity of existing RC T-section beams using CFRP composites", *Cement Concrete Compos.*, **22**(3), 165-174.

Khalifa, A., Gold, W.J., Nanni, A. and MI, A.A. (1998), "Contribution of externally bonded FRP to shear capacity of RC flexural members", *J. Compos. Construct.*, **2**(4), 195-202.

Koutas, L. and Triantafillou, T. (2013), "Use of anchors in shear strengthening of reinforced concrete T-beams with FRP", *J. Compos. Construct.*, **17**(1):101-107.

Lee, J.Y., Hwang, H.B. and Doh, J.H. (2012), "Effective strain of RC beams strengthened in shear with FRP", *Compos. Part B*, **43**, 754-765.

Lees, J.M., Winistörfer, A.U. and Meier, U. (2002), "External prestressed carbon fiber-reinforced polymer strips for shear enhancement of concrete", *J. Compos. Construct.*, **6**(4), 249-256.

Miyauchi, K., Inoue, S., Nishibayashi, S. and Tanaka, Y. (1997), "Shear behaviour of reinforced concrete beam strengthened with CFRP sheet", *Tran. Japan Concrete Inst.*, **19**, 97-104.

Mofidi, A. (2014), "Shear strengthening of RC T-beams using mechanically anchored unbonded dry carbon fiber sheets", *J. Perform. Constr. Facil.*, **24**(1), 31-39.

Monti, G. and Liotta, M.A. (2007), "Tests and design equations for FRP-strengthening in shear", *Constr. Build. Mater.*, **21**(4), 799-809.

Panda, K.C., Bhattacharyya, S.K. and Barai, S.V. (2013), "Shear strengthening effect by bonded GFRP strips and transverse steel on RC T-beams", *Struct. Eng. Mech.*, **47**(1), 75-98.

Sato, Y., Katsumata, H. and Kobatake, Y. (1997), "Shear strengthening of existing reinforced concrete Beams by CFRP sheet", *Proceedings of the 3rd International Symposium on Non-Metallic FRP Reinforcement for Concrete Structures(FRPRCS-3)*, Japan Concrete Institute (JCI), Sapporo, Japan.

Schuman, P.M. (2004), "Mechanical anchorage for shear rehabilitation of reinforced concrete structures with FRP: an appropriate design approach", Ph.D Dessertation, University of California, La Jolla, San Diego.

Taljsten, B. (2003), "Strengthening concrete beam for shear with CFRP sheets", *Constr. Build. Mater.*, **17**(1), 15-26.

TR55 (2012), "Design guidance for strengthening concrete structures using fiber composite material", Technical Report. No. 55, 3rd Edition, The Concrete Society, Camberley, UK.

Triantafillou, T.C. and Antonopoulos, C.P. (2000), "Design of concrete flexural members strengthened in shear with FRP", *J. Compos. Construct.*, **4**(4), 198-205.

Yurdakul, O. and Avsar, O. (2015), "Structural repairing of damaged reinforced concrete beam-column assemblies with CFRPs", *Struct. Eng. Mech.*, **54**(3), 521-543.

Zhou, C.Y., Cheng, X.N. and Hou, Y.B. (2012), "Pilot tests for RC T-beams shear-strengthened with U-shaped CFRP sheets around bars", *Proceedings of The 11th National Conference for Structural Evaluation and Strengthening, Press of Chinese Industry of Building Material*, Taiyuan, China, Augest.

Zhou, C.Y., Ren, D., Liu, J.P. and Xu, P. (2013), "RC T-beams shear-strengthened with CFRP U-strips around bars passing eye bolts penetrating flange", *Proceedings of the Fourth Asia-Pacific Conference on FRP in Structures (APFIS)*, Melbourne, Australia, December.

*CC*